

## The Spatial Distribution of Secondary Electrons Produced in the $\gamma$ -Radiolysis of Water

Ken-ichi KOWARI and Shin SATO

*Department of Applied Physics, Tokyo Institute of Technology, Ookayama, Meguro-ku, Tokyo 152*

(Received October 19, 1977)

The spatial distribution of secondary electrons produced in the  $\gamma$ -radiolysis of water in the liquid phase has been theoretically calculated. The method consists of the combination of the procedure previously developed for the calculation of the  $G$ -value of electrons with the theory proposed by Fröhlich and Platzman for the slowing down of electrons in polar liquids. The  $G$ -value of the ion-pairs initially produced was calculated to be 6.8 on the assumption that the binding energies of electrons in water are equal to those in solid water at 77K. 27% of the ion-pairs were generated in isolated spurs. Another 27% of the ion-pairs were generated in condensed spurs, each of which contains more than one hundred ion-pairs. The other ion-pairs formed less condensed spurs, each of which contains from 2 to 100 ion-pairs. A new definition was given for the classification of spurs: isolated spurs, blobs, and short tracks; the original proposal was by Mozumder and Magee. The diameter of the isolated spur was estimated to be about 100 Å. The distribution of the distance between the parent positive ion and the thermalized electron in the isolated spur was well expressed by the function proposed by Abell and Funabashi, except at very short distances.

When ionizing radiation interacts with a material in the condensed phase, the energy transfer from the radiation to the material occurs through the kinetic energy of the secondary electrons produced, and the energy deposits are heterogeneously distributed in the system. In radiation chemistry, the region in which active species are produced by radiation is called a spur. Mozumder and Magee classified these spurs into three types, on the basis of the amount of energy deposited in the region: isolated spurs, blobs, and short tracks.<sup>1)</sup> Experimentally the distribution of such spurs can be estimated from the number of clusters produced in a cloud chamber. According to the measurement of Wilson, who used 25 keV electrons as the radiation source, 42.6% of the observed clusters contained one ion-pair, 22.5% two pairs, 12.4% three pairs, 10.1% four pairs, and 12.4% more than five pairs.<sup>2)</sup> From the point of view of radiation chemistry, the number of ion-pairs involved in a spur is important, because the reactions occurring in a spur may be dependent upon the number of ion-pairs involved in the spur; for example, the neutralization reaction between positive ions and ejected electrons in a condensed spur may be faster than that in an isolated spur.

We have previously developed a calculation method for the  $G$ -values of ionization and excitation.<sup>3)</sup> Using this method, we can calculate the initial energy distribution of subexcitation electrons. Therefore, if we can estimate the slowing down process of electrons in the condensed phase, we can construct the spatial distribution of secondary electrons produced in the radiolysis. As for the slowing down process of electrons in the condensed phase, Fröhlich and Platzman proposed a theory with which they estimated the rate of slowing down of electrons in water.<sup>4)</sup> Recently Magee and Helman examined this theory numerically and estimated the rates of energy loss of electrons in a few hydrocarbons as well as in water.<sup>5)</sup> As has been stated in their paper, the absolute value of the rate of energy loss is somewhat obscure, because the theory proposed by Fröhlich and Platzman treated only the "indirect" interaction between electrons and surrounding molecules. The treatment of the "direct" interactions, such as the formation

of short-lived negative ions, has not been formulated yet. Consequently, we cannot avoid the appearance of a somewhat arbitrary factor in the estimation of the rate of slowing down of subexcitation electrons.

So far the spatial distribution of secondary electrons has been discussed in connection with the electron scavenging in the  $\gamma$ -irradiated hydrocarbons and with the electric conductivity of the irradiated hydrocarbons. The simplest assumed function was a Gaussian; however, it is now well known that the spatial distribution has a long tail compared with a Gaussian. Freeman and his group used a function which is composed of a Gaussian and a power function.<sup>6)</sup> One of the present authors also discussed the spatial distribution of secondary electrons in the  $\gamma$ -irradiated hydrocarbons and derived a function from the experimental data of the electron scavenging by assuming a diffusion model.<sup>7)</sup> Similar attempts have been made by several investigators.<sup>8)</sup> Among them, Abell and Funabashi proposed a simple exponential function to express the spatial distribution and showed that this function is suitable to explain the experimental data both for the electron scavenging and for the voltage dependence of the electric conductivity of the irradiated hydrocarbons.<sup>9)</sup> However, all of these attempts are empirical and have no rigid theoretical backgrounds. We, therefore, thought that the theoretical derivation of the function expressing the spatial distribution of secondary electrons would be worthwhile carrying out even if several assumptions are involved.

### $G$ -Value of Ionization

*Procedure of Calculation.* When water is exposed to the  $\gamma$ -rays from  $^{60}\text{Co}$ , the energy transfer mainly occurs through the Compton effect. The energy distribution of the Compton electrons can be calculated by using the equation

$$\frac{d\sigma(T)}{dT} = \frac{\pi r_0^2}{\alpha h\nu} \left[ 1 + \frac{T^2}{(h\nu - T)h\nu} + \left\{ 1 - \frac{T}{\alpha(h\nu - T)} \right\}^2 \right], \quad (1)$$

which was derived by Davison and Evans<sup>10)</sup> from the

famous Klein-Nishina formula. Here,  $\sigma(T)$  is the cross section for the formation of Compton electrons with the energy  $T$ ,  $h\nu$  is the energy of the incident  $\gamma$ -rays,  $\alpha = h\nu/mc^2$ , and  $r_0 = e^2/mc^2$ .  $m$  is the mass of electron,  $e$  is the charge, and  $c$  is the velocity of light.

Previously we have calculated the energy distribution of Compton electrons from helium gas irradiated by  $^{60}\text{Co}$   $\gamma$ -rays.<sup>11)</sup> The fraction of the Compton electrons with energy of  $T$  was expressed by  $f(T)$ . This function is common to any material, because Eq. 1 does not discriminate target electrons. The total energy absorbed by the material,  $T_0$ , therefore, is expressed as follows:

$$T_0 = \int_0^{T_{\max}} T f(T) dT. \quad (2)$$

Here,  $T_{\max} = 2\alpha h\nu / (1 + 2\alpha)$ .

Using the function  $f(T)$ , we can calculate the degradation spectrum of the Compton electrons:

$$y_1(T) = \int_T^{T_{\max}} f(T) dT / S(T). \quad (3)$$

$S(T)$  is the stopping power of water and may be expressed as follows:

$$S(T) = N \sum_i n_i \left\{ \int_{E_{si}}^{(T+I_i)/2} E(\sigma_{E,\text{dir}} + \sigma_{E,\text{exc}}) dE + \frac{1}{2} \int_{E_{ti}}^{E_{si}} E \sigma_{E,\text{exc}} dE \right\}. \quad (4)$$

$N$  is the number of molecules in a unit volume,  $n_i$  the number of electrons in the  $i$ -th shell of water,  $I_i$  the binding energy of the electron in the  $i$ -th shell, and  $E_{si}$  and  $E_{ti}$  the energies of the singlet and triplet excitations for the electrons in the  $i$ -th shell.  $\sigma_{E,\text{dir}}$  and  $\sigma_{E,\text{exc}}$  are the differential cross sections of the energy loss  $E$  due to the direct excitation and due to the excitation accompanied with the exchange of electrons, respectively.

In the procedure we developed for the calculation of  $G$ -values, the cross sections of the energy loss are estimated by using the classical binary-encounter-collision theory. For the direct excitation,

$$\sigma_{E,\text{dir}} = \frac{\pi e^4}{T + I_i + E_i} \left( \frac{1}{E^2} + \frac{4E_i}{3E^3} \right), \quad (5)$$

where  $E_i$  is the average kinetic energy of the target electron. For the excitation accompanied with the exchange of electrons,  $E$  in Eq. 5 is replaced by  $T + I_i - E$ .

Once the degradation spectrum of Compton electrons is obtained, we can calculate the degradation spectra of electrons ejected in the later steps of ionization due to the impact of electrons.

$$y_2(T) = \frac{N}{S(T)} \sum_i n_i \int_T^{(T_{\max}-I_i)/2} y_1(T_1) \sigma(T_1 T_2) dT_1 dT_2, \quad (6)$$

$$y_3(T) = \frac{N}{S(T)} \sum_i n_i \int_T^{(T_{\max}-3I_i)/4} y_2(T_1) \sigma(T_1 T_2) dT_1 dT_2. \quad (7)$$

Here,  $\sigma(T_1 T_2)$  is the differential cross section for the production of a secondary electron with energy of

$T_2$  in the collision between the incident electron with energy of  $T_1$  and the target electron in the  $i$ -th shell and is expressed as follows, by using Eq. 5:

$$\sigma(T_1 T_2) = \frac{\pi e^4}{T + I_i + E_i} \left[ \frac{1}{(T_2 + I_i)^2} + \frac{4E_i}{3(T_2 + I_i)^3} + \frac{1}{(T_1 - T_2)^2} + \frac{4E_i}{3(T_1 - T_2)^3} \right]. \quad (8)$$

Equations similar to  $y_2(T)$  and  $y_3(T)$  may be constructed for the later steps. The total degradation spectrum is obviously the sum of the degradation spectra of the electrons ejected in all steps:

$$y(T) = \sum_m y_m(T). \quad (9)$$

The degradation spectrum of electrons is one of the most important values for the irradiated system; from it we can deduce many interesting values concerning the reactions occurring in the system. The  $G$ -value of ionization is one of them.

In order to calculate the  $G$ -value of ionization, we need the total cross section of ionization due to the impact of an electron with the energy  $T$ , which is expressed per target electron as follows:

$$Q_{\text{ion}} = \int_{I_i}^{(T+I_i)/2} (\sigma_{E,\text{dir}} + \sigma_{E,\text{exc}}) dE = \frac{\pi e^4}{T + I_i + E_i} \left[ \left( \frac{1}{I_i} - \frac{1}{T} \right) + \frac{2E_i}{3} \left( \frac{1}{I_i^2} - \frac{1}{T^2} \right) \right]. \quad (10)$$

Then, the number of ions produced by the ejection of the electron in the  $i$ -th shell can be calculated by the equation

$$N_{\text{ion}} = N n_i \int_{I_i}^{T_{\max}} T y(T) Q_{\text{ion}}(T) d \ln T. \quad (11)$$

The  $G$ -value of ionization through this process is obviously

$$G_{\text{ion}} = 100 N_{\text{ion}} / T_0. \quad (12)$$

Similar formulations can be made for other processes, including singlet and triplet excitations.

**Calculated Results.** The constants used for the calculation are summarized in Table 1. Since no experimental values were available, we had to estimate them somewhat arbitrarily. For the binding energies of electrons in water in the liquid phase, we estimated the values from the spectrum of X-ray induced photoelectron spectroscopy obtained with solid state water at 77 K.<sup>12)</sup> The  $E_s$  and  $E_t$  values for the  $1b_1$  orbital are those reported for the gas phase. For other orbitals, the equations shown in the note of Table 1 were used.

TABLE 1. CONSTANTS USED FOR CALCULATION

Orbital	$I_i$	$E_i$	$E_s$	$E_t$
$1b_1$	7.6	45.0	7.42	5.0
$3a_1$	9.8	54.9	9.6 <sup>a)</sup>	7 <sup>b)</sup>
$1b_2$	14.5	74.7	14 <sup>a)</sup>	12 <sup>b)</sup>
$2a_1$	26.3	119	26 <sup>a)</sup>	24 <sup>b)</sup>
$1a_1$	533	1265	533 <sup>a)</sup>	531 <sup>b)</sup>

a)  $E_s = I_i - (I_i - E_s)_{1b_1} = I_i - 0.2$ .

b)  $E_t = I_i - (I_i - E_t)_{1b_1} = I_i - 2.6$ .

TABLE 2. THE  $G$ -VALUES OF IONIZATION AND SINGLET AND TRIPLET EXCITATIONS FROM EACH ORBITAL  
The values in parentheses are the  $G$ -values of superexcited states.

Orbital	$G_o$	$G_s$	$G_t$
1b <sub>1</sub>	3.13	0.23	1.18
3a <sub>1</sub>	1.87	(0.096)	0.15 (0.12)
1b <sub>2</sub>	0.96	(0.075)	(0.018)
2a <sub>1</sub>	0.39	(0.009)	(0.002)
1a <sub>1</sub>	0.008	(5 × 10 <sup>-6</sup> )	(4 × 10 <sup>-7</sup> )

TABLE 3. THE  $G$ -VALUES OF IONIZATION, INCLUDING THE IONIZATION FROM THE SUPEREXCITED STATE ( $G_{ion}$ ) AND OF SINGLET AND TRIPLET EXCITATIONS ( $G_{singlet}$  and  $G_{triplet}$ )

$G_{ion}$	6.76
$G_{singlet}$	0.23
$G_{triplet}$	1.21

In order to estimate the average kinetic energies,  $E_i$ , we deduced an equation:

$$E_i = 9.15I_i^{0.785}, \quad (13)$$

by plotting the reported values of  $E_i$  and  $I_i$  for five noble gases.<sup>13)</sup>

The  $G$ -values calculated are summarized in Table 2. In this Table, the  $G$ -values of the superexcited states which are in the parentheses are involved in those of singlet and triplet excitations. If all of the superexcited states are assumed to be ionized, then the  $G$ -value of ionization should be increased by 0.32. In Table 3 are listed the corrected  $G$ -values.

Since the  $G$ -value of ionization is sensitive to the ionization potential assumed, *i.e.*, the  $I_i$  value for the 1b<sub>1</sub> orbital, we calculated the  $G$ -values by assuming several  $I_i$  values. The results are shown in Fig. 1. The value obtained with  $I_i = 12.6$  eV is that for the gas phase.

### Subexcitation Electrons

**Initial Energy Distribution.** Since the degradation spectrum of electrons in  $\gamma$ -irradiated water has been obtained, the initial energy distribution of subexcitation electrons can be calculated by using the following equations:<sup>14)</sup>

$$N_{sub}(T) = f(T) + N_p(T) + N_c(T); \quad T < E_i, \quad (14)$$

$$N_p(T) = N \sum_i n_i \int_{E_i}^{T+I_i} \gamma(T+E) \sigma(T+E, E) dE,$$

$$N_c(T) = N \sum_i n_i \int_{2T+I_i}^{T_{max}} \gamma(T') \sigma(T', T+I_i) dT'.$$

The first term,  $f(T)_{T < E_i}$ , represents the contribution of Compton electrons and is negligibly small compared with the second and third terms when the energy of the incident  $\gamma$ -rays is higher than the binding energy of the electron in the innermost shell. The second term corresponds to the electrons which had the energy higher than the threshold,  $E_i(1b_1)$  in the present case, before the last collision. We may call them "parent"

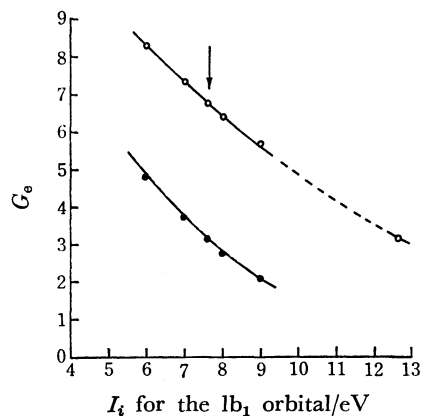


Fig. 1. The calculated  $G$ -value of electrons as a function of the energy assumed for the electron in the 1b<sub>1</sub> orbital. O, for the total; ●, for the  $G$ -value from the 1b<sub>1</sub> orbital only. The arrow shows the value used in the following calculation.

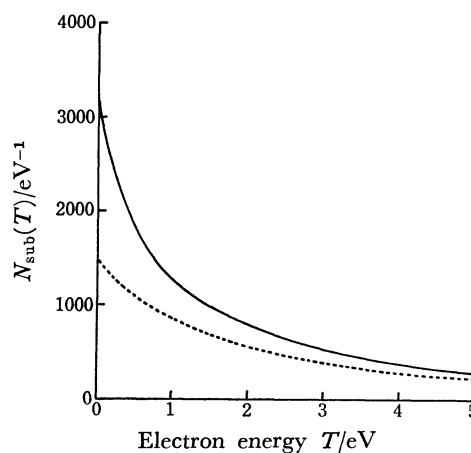


Fig. 2. The initial energy distribution of subexcitation electrons. Solid line is for the total and dotted line for the "child" electrons.

electrons. The third term represents the electrons generated in the last collision with the energy lower than  $E_i(1b_1)$ , which we may call "child" electrons.

Figure 2 shows the calculated result for the initial energy distribution of subexcitation electrons produced in water. The dotted curve corresponds to the "child" electrons. The number of "child" electrons is about twice that of "parent" electrons. Douthat calculated the energy distribution of subexcitation electrons in helium gas irradiated by 1.99 keV electrons.<sup>14)</sup> The curve reported is similar to that shown in Fig. 2.

If the irradiated material is in the gas phase at a low pressure, these subexcitation electrons are homogeneously distributed in the material and collide with the surrounding molecules to excite their vibrations and rotations. The rate of the energy loss, however, is much slower than that due to electronic excitations when the electron energy is higher than the threshold.<sup>15)</sup>

**Thermalization Distance.** According to the theory proposed by Fröhlich and Platzman, the rate of the energy loss of an electron in the 1–10 eV energy region due to dielectric relaxation is expressed by this equation:

$$-\frac{dT}{dt} = \frac{2e^2}{\pi v} \int_0^\infty \frac{\omega \varepsilon^2(\omega)}{\varepsilon_1^2(\omega) + \varepsilon_2^2(\omega)} x K_0(x) K_1(x) dx. \quad (15)$$

Here  $v$  is the velocity of the moving electron,  $x$  is defined by  $x = \omega b_{\min}/v$ ,  $\omega/2\pi$  is the frequency,  $b_{\min}$  is the minimum value of the collision parameter,  $\varepsilon_1$  and  $\varepsilon_2$  are the real and imaginary part of the complex dielectric constant of the solvent, and  $K_0$  and  $K_1$  are the modified Bessel functions of the second kind, of order 0 and 1. In the case of polar solvents such as water, the dipolar relaxation is the main process for the energy loss and the rate of energy loss can be approximated as follows:

$$-\frac{dT}{dt} \simeq \frac{\pi e^2}{4d} \frac{\varepsilon_s - \varepsilon_{ir}}{\tau n^4}. \quad (16)$$

Here  $d$  is the intermolecular distance,  $\tau$  the relaxation time,  $n$  the refractive index,  $\varepsilon_s$  the static dielectric constant, and  $\varepsilon_{ir}$  the dielectric constant at frequencies lower than the lowest main infrared absorption frequency.

Fröhlich and Platzman substituted the experimental values of water at 20 °C into Eq. 16 and obtained  $10^{13} \text{ eV s}^{-1}$  for  $-dT/dt$ .

Magee and Helman recently discussed Eq. 15 and calculated the rate of energy loss of subexcitation electrons in benzene and polyethylene, which have no dipole moments, as well as in water. The rates of the energy loss calculated in benzene and polyethylene were a little smaller than that in water.

As stated in the Introduction, the theory of Fröhlich and Platzman treats only the "indirect" interaction of moving electrons with surrounding molecules. Magee and Helman estimated the rate of the energy loss due to the "direct" interaction in water and suggested that  $-dT/dt \simeq 10^{14} \text{ eV s}^{-1}$ . In the present calculation, therefore, we used two values,  $10^{13}$  and  $10^{14} \text{ eV s}^{-1}$  for  $-dT/dt$ .

If the rate of energy loss is independent of the electron energy, the path length over which an electron with the energy  $T$  loses energy down to  $T_{\min}$  may be calculated by the equation

$$R = \frac{2}{3} \left( \frac{2}{m} \right)^{1/2} \frac{1}{k} [T^{3/2} - T_{\min}^{3/2}], \quad (17)$$

where  $m$  is the electron mass and  $k$  is the rate of energy loss.

The relation between the crooked path,  $R$ , and the straight distance,  $r$ , between the starting point and the point where the electron energy is degraded to  $T_{\min}$  can be given by the theory of random walks.<sup>16)</sup> With given  $R$ , the distribution in  $r$ , *i.e.*, the probability of arriving at a point  $r$ ,  $P(r)$ , is given by

$$P(r) = 4\pi r^2 W(r) \quad (18)$$

and

$$W(r) = (2\pi RL/3)^{-3/2} \exp(-3r^2/2RL). \quad (19)$$

Here  $L$  is the mean free path of an electron in the solvent.

As will be discussed later, about 30% of the ion-pairs produced in the  $\gamma$ -irradiated water are generated in isolated spurs. The electrons in these do not interact with active species in other spurs before they are thermalized, and the initial energy distribution of electrons in the isolated spurs are similar to that of the "child" electrons discussed above. Consequently, the spatial

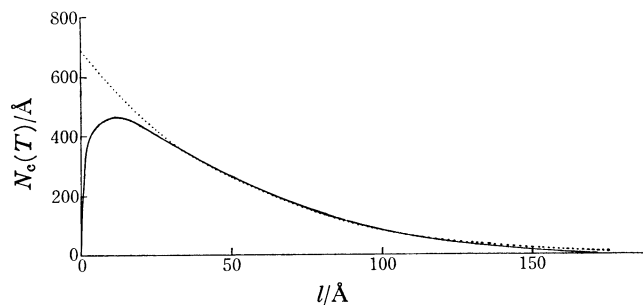


Fig. 3. The spatial distribution of thermalized electrons in the isolated spurs.  $-dT/dt = 10^{13} \text{ eV s}^{-1}$ . For the dotted line, see the Text.

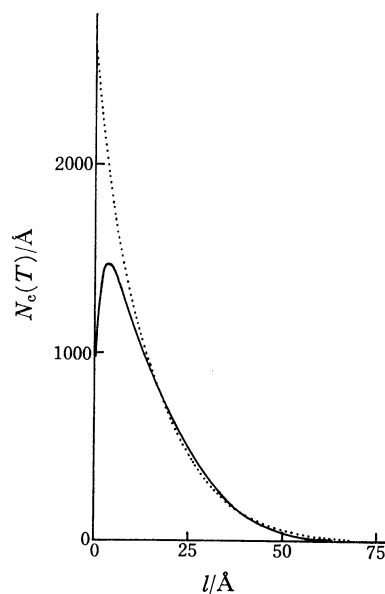


Fig. 4. The spatial distribution of thermalized electrons in the isolated spurs.  $-dT/dt = 10^{14} \text{ eV s}^{-1}$ . For the dotted line, see the Text.

distribution of electrons when they are thermalized in the isolated spurs can be expressed by

$$F(r) = \int_0^{E_i} W(r) N_e(T) dT. \quad (20)$$

Here,  $T_{\min}$  should be taken as thermal energy.

For the actual calculation, we took,  $L = 3 \text{ Å}$  and  $T_{\min} = 0$ . The calculated results are shown in Figs. 3 and 4, where the rate of energy loss  $k$  is assumed to be  $10^{13}$  and  $10^{14} \text{ eV s}^{-1}$ , respectively. The dotted lines shown in both figures are drawn by using the function  $4\pi r^2 F(r) = A \exp(-r/b)$ ;  $A = 690$  and  $b = 48 \text{ Å}$  for Fig. 3 and  $A = 3000$  and  $b = 14 \text{ Å}$  for Fig. 4. Except for the very small value of  $r$ , both curves coincide with those theoretically estimated.

### The Number of Ion-pairs in a Spur

The energy of the secondary electrons ejected from the parent molecules into the solvent ranges from zero to the maximum value,  $T_{\max}$ . If the initial energy is low, the electron will be thermalized close by the parent molecule ion and will make an ion-pair.

The initial energy distribution of secondary electrons

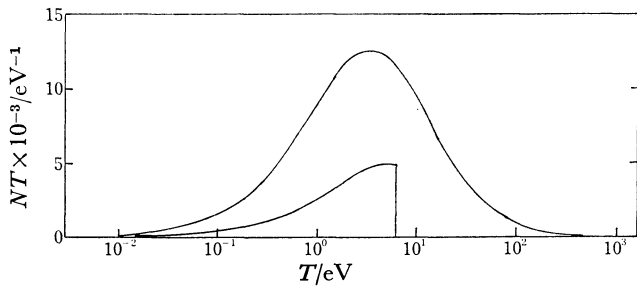


Fig. 5. The initial energy distribution of secondary electrons. The lower curve is for the subexcitation electrons in the isolated spurs.

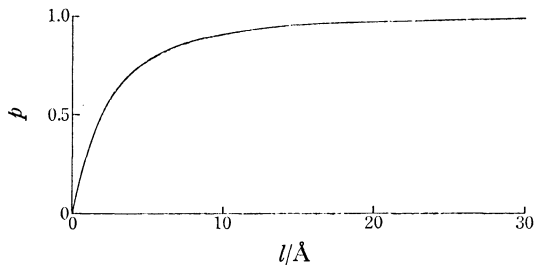


Fig. 6. The distance between two successive ionizations occurring in the  $\gamma$ -irradiated water.

can be calculated also from the degradation spectrum obtained above:

$$N(T) = f(T) + N \sum_i n_i \int_{T+I_i}^{T_{\max}} \mathcal{P}(T') \sigma(T', T) dT', \quad (21)$$

where  $f(T)$  is the contribution of Compton electrons.  $\sigma(T', T)$  is the differential cross section which appears in Eq. 8. The calculated result for the secondary electrons in the  $\gamma$ -irradiated water is shown in Fig. 5. Here the relation  $TN(T)$  vs.  $\ln T$  is plotted, so that the area under the curve is proportional to the number of secondary electrons. The electrons whose energy is higher than the threshold,  $E_i$ , correspond to the "parent" electrons discussed in the previous section and the electrons whose energy is lower than  $E_i$  are the "child" electrons.

If a "parent" electron has a higher energy than the ionization potential of water, it will give rise to another ionization. The number of the "child" electrons produced in this second ionization has already been counted in Fig. 5. The average probability with which "parent" electrons give rise to such ionizations within the distance,  $l$ , from the last ionization is expressed by the following equation:

$$p = \frac{\int_I^{T_{\max}} [1 - \exp(-N \sum_i n_i Q_i(T) l)] N(T) dT}{\int_I^{T_{\max}} N(T) dT}. \quad (22)$$

Here  $Q_i(T)$  is the total ionization cross section due to a "parent" electron with the energy  $T$ . The values of  $p$  are plotted in Fig. 6 as a function of the distance  $l$ . Obviously, most of "parent" electrons in the  $\gamma$ -irradiated water give rise to their second ionizations very close to the first ionizations.

As has been shown in the previous section, if two

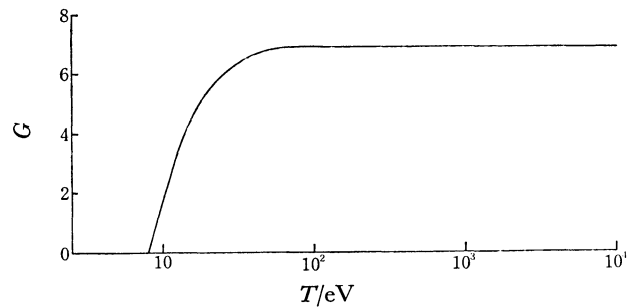


Fig. 7. The  $G$ -value of electrons as a function of the energy of the incident electron.

successive ionizations occur within a short distance—let us take 150 Å as the upper limit—the two ion-pairs produced may interact with each other during their thermalization; *i.e.*, these two ion-pairs may be regarded to be in the same spur.

The energy of a "parent" electron which induces two successive ionizations within the interval of 150 Å on the average corresponds to 10 keV. Consequently, if a "parent" electron has the energy higher than 10 keV, "child" electrons produced by this "parent" electron will be isolated from other ionizations. In Fig. 5, the initial energy distribution of "child" electrons in isolated spurs is also plotted. If we plot these values in Fig. 2, the curve obtained is similar to that for  $N_e$ . The percentage of the "child" electrons in isolated spurs against the total electrons has been calculated to be 27%.

If the energy of "parent" electrons is lower than 10 keV and sufficiently higher than the ionization potential of water, these electrons will produce condensed spurs, and if the energy of "parent" electrons is a little higher than the ionization potential of water, the spurs generated will contain a few ion-pairs.

In order to calculate the number of ion-pairs in spurs, we need the relationship between the  $G$ -value of electrons and the energy of the incident electron. This type of calculation has already been made for helium gas.<sup>11)</sup> Figure 7 is the result for water in the liquid phase. By combining this result with the number of "parent" electrons, we can calculate the number of ion-pairs produced in each spur. The calculated numbers, however, are not always integers. Therefore, we tentatively allotted the numbers proportionally to the adjacent integral numbers; for example, when the number was 2.6, we read it as 40% for two ion-pairs and 60% for three ion-pairs. The results thus calculated are summarized in Tables 4 and 5.

Table 4 shows the percentage of the number of spurs which contain different numbers of ion-pairs against the total number of spurs. This result may be compared with the observation of Wilson discussed in the Introduction. Similar observations have been made by Beekman with electrons at higher energies.<sup>17)</sup> Both observations are included in Table 4.

On the other hand, Table 5 shows the distribution of ion-pairs in the spurs of different types. It is noticeable that 27% of the ion-pairs are generated in isolated spurs and another 27% of the ion-pairs are generated in very condensed spurs which consist of more than one

TABLE 4. CALCULATED RELATIVE FREQUENCIES OF SPURS IN WATER AND RELATIVE FREQUENCIES OF CLUSTERS OBSERVED IN A CLOUD CHAMBER

Ion-pairs per spur	1	2	3	4	>4
Relative frequency %	73.6	11.7	5.0	3.1	6.6
Ion-pairs per cluster	1	2	3	4	>4
Relative frequency %					
Source: 25 keV <sup>2)</sup>	42.6	22.5	12.4	10.1	12.4
150 keV <sup>17)</sup>	60	23	8	4	5
320 keV <sup>17)</sup>	62	20	9	4	5

TABLE 5. RELATIVE NUMBERS OF ION-PAIRS IN DIFFERENT SPURS

Ion-pairs per spur	Relative number %	
1	26.8	Isolated spurs
2	8.5	
3	5.4	
4	4.5	
5—10	10.9	Blobs
11—100	16.5	
101—	27.4	Short tracks

hundred ion-pairs.

Mozumder and Magee classified spurs into three types: isolated spurs, blobs, and short tracks, on the basis of the energy deposited in them. A similar classification may be applied to the result shown in Table 5: *i.e.*, isolated spurs for the spurs containing only one ion-pair, blobs for the spurs containing two to ten ion-pairs, and short tracks for the spurs containing more than ten ion-pairs.

### Discussion

*G-Value of Electrons.* Figure 8 shows the contribution of different portions of the electron degradation spectrum to the ionization and excitations, singlet and triplet, induced by one keV electrons in water. This type of figure has already been discussed in previous papers.<sup>3,11)</sup> From this figure, we can estimate the number of ionizations and excitations during the slowing down of the incident electron.

Let us consider the track of ionizations in water induced by a 1keV electron. Since the ionization probability along the path of a high energy electron is roughly proportional to the reciprocal of the electron energy, the average distance between two successive ionizations near the starting point is about 15 Å. The direction of the path will not be changed so often, because the cross section for small energy loss, around 10 eV, is much larger than that for the larger energy loss. After having induced about 20 ionizations and a few electronic excitations, the energy of the "parent" electron is degraded to 500 eV, a value which is comparable to the binding energy of the electrons in the inner-most shell. After the electron energy reached 500 eV, the path of the "parent" electron may change direction often. The average interval of two successive ionizations is now 9 Å, a distance which corresponds to three times the diameter of a water molecule. Con-

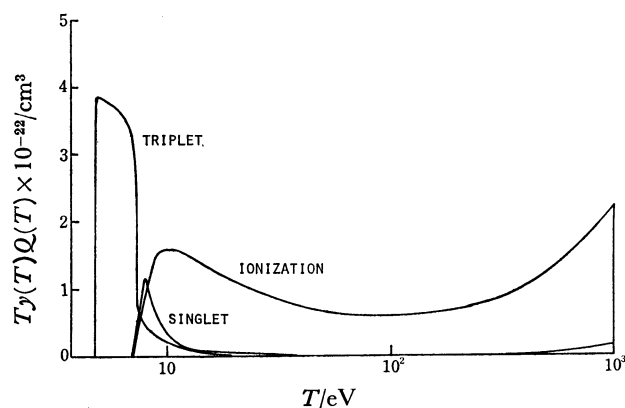


Fig. 8. The contribution of the different portions of the electron degradation spectrum to ionization and singlet and triplet excitations.

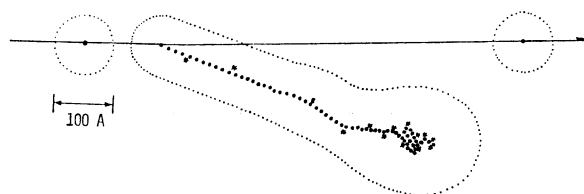


Fig. 9. A schematic picture of an example of short tracks produced by a 1 keV electron. A dot corresponds to an ionization and an asterisk to an excitation.

sequently, about 50 ion-pairs may be produced in a very small space at the end of the track of ionizations. Since the diameter of the isolated spur is about 100 Å, as shown in Fig. 3, the density of charged species at the end of the track must be very high. A schematic picture of a short track is shown in Fig. 9.

According to the measurement of Hunt *et al.*, the initial *G*-value of dry electrons in water is 4.8.<sup>18)</sup> They used one mol l<sup>-1</sup> cadmium ions as the scavenger for electrons. This concentration corresponds to one scavenger ion per 55 water molecules. At the end of the track of a high energy electron, the density of ion-pairs must be comparable to or higher than that of scavenger ions. A large part of the electrons, a percentage which we cannot calculate at present, may escape from the scavenging and be neutralized with their counter ions. Consequently, we do not think that the value *G*<sub>0</sub>=6.8 obtained in the present calculation is absurdly large.

*The Rate of Slowing Down of Subexcitation Electrons.* For the rate of slowing down of subexcitation electrons, we took two values, 10<sup>13</sup> and 10<sup>14</sup> eV s<sup>-1</sup>. These values are somewhat arbitrary, as was stated when we introduced them. If more reliable values become available, these values should be replaced by them. Another point important for the present calculation is the assumption that the rate of energy loss is independent of the electron energy. This assumption might be acceptable for the energy loss due to the "indirect" interaction, but since the "direct" interaction is a kind of resonance effect, the rate of the energy loss must be strongly dependent on the electron energy. Although this process has not been formulated yet, it may be better for the calculation to treat the "direct" interaction as if it were a kind of

electronic excitation.

In the present calculation, only one value of the rate of energy loss has been assumed for all subexcitation electrons ranging from thermal energy to the maximum,  $E_t$ . However, when the electron energy is degraded to subvibrational energy ( $\approx 0.4$  eV), no process of the energy loss but that due to the intermolecular vibrations remains. In a polar solvent, such a slow electron may be solvated by surrounding molecules. In non-polar solvents, however, these electrons may migrate further into the solvent, as suggested by Hummel *et al.*<sup>19)</sup> and estimated by Mozumder and Magee.<sup>20)</sup>

According to the estimate of Mozumder and Magee, the thermalization distance of the subvibrational electrons in hexane is in the order of 50 Å, a distance which is of the same order as that estimated here to be the thermalization distance of the subexcitation electrons.

*Spatial Distribution of Ion-pairs in Spurs.* Most of electrons and positive ions generated in blobs and short tracks may be neutralized pairwise before they are thermalized. If the concentration is low, electron scavengers can capture only electrons which have escaped the neutralization. The spatial distribution function of ion-pairs derived for the interpretation of the experimental results of electron scavenging and of electric conductivity is, therefore, composed of the sum of two parts: one is the distribution of ion-pairs in isolated spurs and the other is the distribution of ion-pairs which have escaped the neutralization in blobs and short tracks.

As has been shown in the Results section, the spatial distribution of ion-pairs in isolated spurs was well expressed by the function proposed by Abell and Funabashi. However, we think that this agreement resulted from a somewhat fortuitous cancellation.

Let us assume that only one ion-pair is left after the neutralization in each blob and short track. Then, all spurs now contain only one ion-pair, the  $G$ -value of which is 2.5 ( $\approx 6.8 \times 26.8 / 73.6$ ). As Table 4 shows, 74% of them come from the original isolated spurs and the rest, 26%, from blobs and short tracks. Although we cannot calculate it numerically, the spatial distribution of ion-pairs which have escaped the neutralization in blobs and short tracks may be much broader than that in the original isolated spurs. If we take this contribution into account, the spatial distribution should have a long tail.

On the other hand, the function of Abell and Funabashi has been proposed to explain the experiments

carried out with hydrocarbons, in which the thermalization of subvibration electrons has to be considered. As Mozumder suggested,<sup>21)</sup> the spatial distribution of electrons during the degradation of subvibrational energies is getting close to a Gaussian, which is sharper than the function of Abell and Funabashi. This effect might cancel the broader distribution of ion-pairs which escaped the neutralization in blobs and short tracks.

## References

- 1) A. Mozumder and J. L. Magee, *Radiat. Res.*, **28**, 203 (1966).
- 2) C. T. R. Wilson, *Proc. R. Soc. London, Ser. A*, **104**, 1, 192 (1923).
- 3) S. Sato, K. Okazaki, and S. Ohno, *Bull. Chem. Soc. Jpn.*, **47**, 2174 (1974).
- 4) H. Fröhlich and R. L. Platzman, *Phys. Rev.*, **92**, 1152 (1953).
- 5) J. L. Magee and W. P. Helman, *J. Chem. Phys.*, **66**, 310 (1977).
- 6) J.-P. Dodelet, K. Shinsaka, U. Kortsch, and G. R. Freeman, *J. Chem. Phys.*, **59**, 2376 (1973).
- 7) S. Sato and T. Oka, *Bull. Chem. Soc. Jpn.*, **44**, 856 (1971).
- 8) M. Tachiya, *J. Chem. Phys.*, **56**, 4377 (1972); M. Baba and K. Fueki, *Bull. Chem. Soc. Jpn.*, **48**, 2240 (1975).
- 9) G. C. Abell and K. Funabashi, *J. Chem. Phys.*, **58**, 1079 (1973).
- 10) C. M. Davison and R. D. Evans, *Rev. Mod. Phys.*, **24**, 79 (1952).
- 11) S. Sato, K. Kowari, and K. Okazaki, *Bull. Chem. Soc. Jpn.*, **49**, 933 (1976).
- 12) K. Siegbahn *et al.*, "ESCA Applied to Free Molecules," North-Holland, Amsterdam (1971).
- 13) Y.-K. Kim, *Radiat. Res.*, **61**, 21 (1975); private communication.
- 14) D. A. Douthat, *Radiat. Res.*, **61**, 1 (1975).
- 15) M. Inokuti, *Rev. Mod. Phys.*, **43**, 297 (1971).
- 16) S. Chandrasekhar, *Rev. Mod. Phys.*, **15**, 1 (1943).
- 17) W. J. Beekman, *Physica*, **15**, 327 (1949); A. Ore and A. Larsen, *Radiat. Res.*, **21**, 331 (1964).
- 18) J. W. Hunt, "Advances in Radiation Chemistry," ed by M. Burton and J. L. Magee, John Wiley & Sons, Vol. 5, New York (1976), p. 185.
- 19) A. Hummel, A. O. Allen, and F. H. Watson, Jr., *J. Chem. Phys.*, **44**, 3431 (1966).
- 20) A. Mozumder and J. L. Magee, *J. Chem. Phys.*, **47**, 939 (1967).
- 21) A. Mozumder, "Advances in Radiation Chemistry," ed by M. Burton and J. L. Magee, John Wiley & Sons, Vol. 1, New York (1969), p. 1.